

# THE NFW DARK MATTER DENSITY PROFILE LEADS TO AXIALLY SYMMETRIC VELOCITY DISTRIBUTION-IMPLICATIONS ON DIRECT DARK MATTER SEARCHES

J.D. Vergados

*University of Ioannina, Ioannina, GR 45110, Greece \**

In the present paper we obtain the WIMP velocity distribution in our vicinity starting from spherically symmetric WIMP density profiles in a self consistent way by employing the Eddington approach. By adding a reasonable angular momentum dependent term in the expression of the energy, we obtain axially symmetric WIMP velocity distributions as well. We find that some density profiles lead to approximate Maxwell-Boltzmann distributions, which are automatically defined in a finite domain, i.e. the escape velocity need not be put by hand. The role of such distributions in obtaining the direct WIMP detection rates, including the modulation, is studied in some detail and, in particular, the role of the asymmetry is explored.

PACS numbers: 95.35.+d, 12.60.Jv

## INTRODUCTION

The combined MAXIMA-1 [1], BOOMERANG [2], DASI [3] and COBE/DMR Cosmic Microwave Background (CMB) observations [4] imply that the Universe is flat [5],  $\Omega = 1.11 \pm 0.07$  and that most of the matter in the Universe is Dark [6]. i.e. exotic. Combining the WMAP data with other experiments, crudely speaking one finds:

$$\Omega_b = 0.05, \Omega_{CDM} = 0.30, \Omega_\Lambda = 0.65$$

Since the non exotic component cannot exceed 40% of the CDM [7], there is room for the exotic WIMP's (Weakly Interacting Massive Particles). Supersymmetry naturally provides candidates for the dark matter constituents [8]-[9]. In the most favored scenario of supersymmetry the LSP (Lightest Supersymmetric Particle) can be simply described as a Majorana fermion, a linear combination of the neutral components of the gauginos and higgsinos [8]-[10]. In most calculations the neutralino is assumed to be primarily a gaugino, usually a bino. Even though there exists firm indirect evidence for a halo of dark matter in galaxies from the observed rotational curves, it is essential to directly detect [8]-[11] such matter. Until dark matter is actually detected, we shall not be able to exclude the possibility that the rotation curves result from a modification of the laws of nature as we currently view them. This makes it imperative that we invest a maximum effort in attempting to detect dark matter whenever it is possible. Furthermore such a direct detection will also unravel the nature of the constituents of dark matter.

The possibility of such detection, however, depends on the nature of the dark matter constituents (WIMPs). Since the WIMP is expected to be very massive,  $m_\chi \geq 30 GeV$ , and extremely non relativistic with average kinetic energy  $T \approx 50 KeV (m_\chi/100 GeV)$ , it can be directly detected [8]-[11] mainly via the recoiling of a nucleus (A,Z) in elastic scattering. The event rate for such a process can be computed from the following ingredients:

1. An effective Lagrangian at the elementary particle (quark) level obtained in the framework of supersymmetry as described , e.g., in Refs [10, 12].
2. A well defined procedure for transforming the amplitude obtained using the previous effective Lagrangian from the quark to the nucleon level, i.e. a quark model for the nucleon. This step is not trivial, since the obtained results depend crucially on the content of the nucleon in quarks

---

\* e-mail: vergados@cc.uoi.gr

other than u and d. This is particularly true for the scalar couplings, which are proportional to the quark masses [13]–[14], [15] as well as the isoscalar axial coupling [15, 16].

3. Knowledge of the relevant nuclear matrix elements [17]–[18], obtained with as reliable as possible many body nuclear wave functions. Fortunately in the case of the scalar coupling, which is viewed as the most important, the situation is a bit simpler, since then one needs only the nuclear form factor.
4. Knowledge of the WIMP density in our vicinity and its velocity distribution. Since the essential input here comes from the rotational curves, dark matter candidates other than the LSP (neutralino) are also characterized by similar parameters.

In the past various velocity distributions have been considered. The one most used is the isothermal Maxwell-Boltzmann velocity distribution with  $\langle v^2 \rangle = (3/2)v_0^2$  where  $v_0$  is the velocity of the sun around the galaxy, i.e. 220 km/s. Extensions of this M-B distribution were also considered, in particular those that were axially symmetric with enhanced dispersion in the galactocentric direction [19, 20]. In such distributions an upper cutoff  $v_{esc} = 2.84v_0$  was introduced by hand. In a different approach Tsallis type functions, derived from simulations of dark matter densities were employed, see e.g. recent calculations [21] and references there in .

Non isothermal models have also been considered. Among those one should mention the late infall of dark matter into the galaxy, i.e caustic rings [22, 23, 24, 25, 26], dark matter orbiting the Sun [27], Sagittarius dark matter [28].

The correct approach in our view is to consider the Eddington proposal [29], i.e. to obtain both the density and the velocity distribution from a mass distribution, which depends both on the velocity and the gravitational potential. Our motivation in using Eddington [29] approach to describing the density of dark matter is found, of course, in his success in describing the density of stars in globular clusters. Since this approach adequately describes the distribution of stars in a globular cluster in which the main interaction is gravitational and because of its generality , we see no reason why such an approach should not be applicable to dark matter that also interact gravitationally. It seems, therefore, not surprising that this approach has been used by Merritt [30] and applied to dark matter by Ullio and Kamionkowski[31] and more recently by us [32],[33].

It is the purpose of the present paper to extend the previous work and obtain a dark matter velocity distribution, which need not be spherically symmetric, consistent with assumed halo matter distributions with a natural upper velocity cut off. It will then be shown that this distribution can be approximated by a Maxwell-Boltzmann (M-B) distribution with a finite domain that depends on the asymmetry parameter. The distribution obtained will be used to calculate WIMP direct detection rates including the annual modulation, as a function of the asymmetry parameter.

## THE DARK MATTER DISTRIBUTION IN THE CONTEXT OF THE EDDINGTON APPROACH

As we have seen in the introduction the matter distribution can be given[33] as follows

$$dM = 2\pi f(\Phi(\mathbf{r}), v_r, v_t) dx dy dz v_t dv_t dv_r \quad (1)$$

where the function  $f$  the distribution function, which depends on  $\mathbf{r}$  through the potential  $\Phi(\mathbf{r})$  and the tangential and radial velocities  $v_t$  and  $v_r$ . We will limit ourselves in spherically symmetric systems. Then the density of matter  $\rho(|r|)$  satisfies the equation:

$$d\rho = 2\pi f(\Phi(|\mathbf{r}|), v_r, v_t) v_t dv_t dv_r \quad (2)$$

The distribution is a function of the total energy:

- The energy  $E$  is  $\Phi(r) + \frac{v^2}{2}$ . Then

$$\rho(r) = 4\pi \int f(\Phi(r) + \frac{v^2}{2})v^2 dv = 4\pi \int_{\Phi}^0 f(E)\sqrt{2(E - \Phi)}dE \quad (3)$$

This is an integral equation of the Abel type. It can be inverted to yield:

$$f(E) = \frac{\sqrt{2}}{4\pi^2} \frac{d}{dE} \int_E^0 \frac{d\Phi}{\sqrt{\Phi - E}} \frac{d\rho}{d\Phi} \quad (4)$$

The above equation can be rewritten as:

$$f(E) = \frac{1}{2\sqrt{2}\pi^2} \left[ \int_E^0 \frac{d\Phi}{\sqrt{\Phi - E}} \frac{d^2\rho}{d\Phi^2} - \frac{1}{\sqrt{-E}} \frac{d\rho}{d\Phi} \Big|_{\Phi=0} \right] \quad (5)$$

In order to proceed it is necessary to know the density as a function of the potential. In practice only in few cases this can be done analytically. This, however, is not a problem, since this function can be given parametrically by the set  $(\rho(r), \Phi(r))$  with the position  $r$  as a parameter. The potential  $\Phi(r)$  for a given density  $\rho(r)$  by solving Poisson's equation.

Once the function  $f(E)$  is known we can obtain the needed velocity distribution in our vicinity ( $r = r_s$ ) by writing:

$$f_d(v) = f(\Phi(r)|_{r=r_s} + \frac{v^2}{2}) \quad (6)$$

The resulting function must be suitably normalized.

- We suppose now that there is an additional kinetic term associated with an angular momentum [34], i.e. :

$$E = \Phi(r) + \frac{v^2}{2} + \frac{|r \times v|^2}{2r_0^2} = \Phi(r) + \frac{v^2}{2} + \frac{r^2}{2r_0^2} v_t^2 = \Phi(r) + \frac{v_r^2}{2} + (1 + \frac{r^2}{r_0^2}) \frac{v_t^2}{2} \quad (7)$$

where  $v_r$  and  $v_t$  are the radial, i.e. outwards from the center of the galaxy, and the tangential components of the velocity and  $r_0$  is the "radius of inertia" to be treated as a phenomenological parameter. We now have:

$$d\rho = 2\pi \int f \left( \Phi(\mathbf{r}) + \frac{v_r^2}{2} + (1 + \frac{r^2}{r_0^2}) \frac{v_t^2}{2} \right) v_t dv_t dv_r \quad (8)$$

The last integral takes the form:

$$\rho(r) = 4\pi \left( 1 + \frac{r^2}{r_0^2} \right) \int_{\Phi}^0 f(E) \sqrt{2(E - \Phi)} dE \quad (9)$$

This equation is the same with Eq. (3) with the understanding that

$$\rho(\Phi) \rightarrow \tilde{\rho}(\Phi) = \rho(\Phi) / \left( 1 + \frac{\tilde{r}^2(\phi)}{r_0^2} \right) \quad (10)$$

The function  $\tilde{r}(\Phi)$  can be obtained by inverting the equation  $\Phi = \Phi(r)$ . In practice this is not needed, if, as we have mentioned above, we use  $r$  as a parameter. We thus find:

$$f(E) = \frac{1}{2\sqrt{2}\pi^2} \left[ \int_E^0 \frac{d\Phi}{\sqrt{\Phi - E}} \frac{d^2\tilde{\rho}}{d\Phi^2} - \frac{1}{\sqrt{-E}} \frac{d\tilde{\rho}}{d\Phi} \Big|_{\Phi=0} \right] \quad (11)$$

The velocity distribution in our vicinity becomes

$$f_d(v) = f(\Phi(r)|_{r=r_s} + \frac{v^2}{2} + (1 + \frac{r_s^2}{r_0^2}) \frac{v_t^2}{2}) \quad (12)$$

and is only axially symmetric.

The characteristic feature of this approach is that the velocity distribution vanishes outside a given region specified by a cut off velocity  $v_m$ , by the positive root of the equation  $f_d(v) = 0$

## SIMPLE REALISTIC DARK MATTER DENSITY PROFILES

There are many halo density profiles, which have been employed. Among the most commonly used are:

- The VO density profile [33]

$$\rho(x) = \rho_0 \left( \begin{array}{l} \frac{1}{1+x^2}, \quad x \leq c \\ \left( \frac{2(c^2+1)}{(x^2+1)^2} - \frac{(c^2+1)^2}{(x^2+1)^3} \right), \quad x > c \end{array} \right) \quad (13)$$

with  $a$  the radius of the Galaxy. The distance  $c$  is very large, so that the the rotational velocity remains essentially constant with the distance from the center of the galaxy even at quite large distances. The above form was taken by the requirement that at  $x = c$  the density is continuous with a continuous derivative. This will be referred to as VO profile.

The potential in the region  $x < c$  is given by:

$$\frac{\Phi_{<}(x)}{\Phi_0} = I_{<}(x) + c_3 \quad (14)$$

The solution in the outer region takes the form:

$$\frac{\Phi_{>}(x)}{\Phi_0} = I_{<}(c) + I_{>}(x) - I_{>}(c) + c_3 \quad (15)$$

where the constant  $c_3$  can be chosen to make the potential vanish at infinity and

$$I_{<} = \frac{\tan^{-1}(x)}{x} + \frac{1}{2} \log(x^2 + 1) \quad (16)$$

$$I_{>} = \frac{1}{8} \left( \frac{(c^2 + 1)^2}{x^2 + 1} + \frac{(c^2 - 7) \tan^{-1}(x) (c^2 + 1)}{x} + \frac{(-c^4 + 6c^2 + 15) \tan^{-1}(c) - c(c^2 + 15)}{x} \right) \quad (17)$$

by choosing  $c_3$  as

$$c_3 = \frac{1}{4} (2 \log(c^2 + 1) + 7)$$

the potential can be made to vanish at infinity. The density is shown in Fig. 1 and the obtained potential is shown in Fig. 2 .

- Another simple profile is:

$$\rho(x) = \frac{\rho_0}{x(1+x)^2}, \quad x = \frac{r}{a} \quad (18)$$

known as NFW distribution [35],[31], which has been suggested by N-body simulations . This profile provides a better description of the expected density near the center of the galaxy. It does not, however, predict the constancy of the rotational velocities at large distances. The density is shown in Fig. 3 and the obtained potential is shown in Fig. 4 .

The obtained rotational velocity curve, due to dark mater alone, is given in Fig. 5 in units of  $\sqrt{4\pi G_N a^2 \rho_0}$ . One can obtain the value of  $\rho_0$  by fitting the rotational velocity in our vicinity to the sun's rotational velocity  $220 \text{ km s}^{-1}$ . We find  $0.3$  and  $0.5 \text{ GeV/cm}^3$  for the VO and NFW profiles respectively. As we have seen above the dependence of the density on the potential is much more interesting. With thus show these functions in Figs 6 and 7.

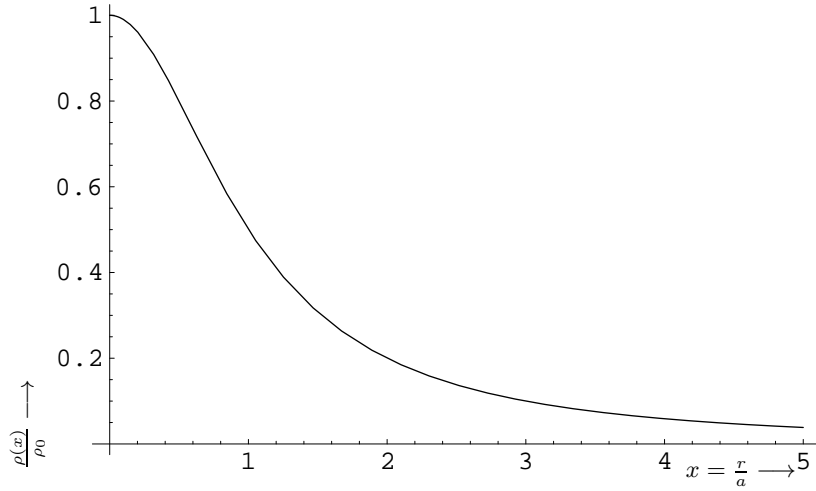


FIG. 1: The VO dark matter density distribution in dimensionless units.

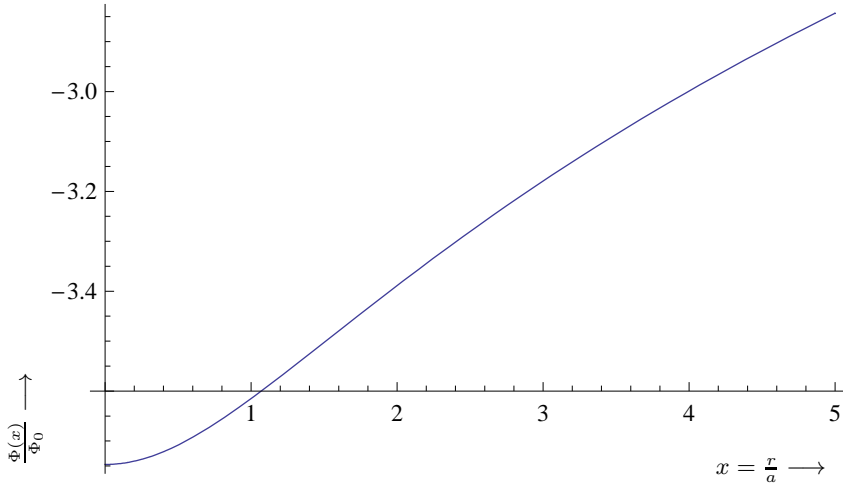


FIG. 2: The potential  $\frac{\Phi(x)}{\Phi_0}$ ,  $\Phi_0 = 4\pi G_N a^2 \rho_0$ , obtained with the VO density function shown in Fig. 1 and chosen to vanish at infinity. This potential drops to zero at infinity but this happens quite slowly.

### VELOCITY DISTRIBUTIONS

Before proceeding further we define the asymmetry in the usual way:

$$\beta = 1 - \frac{v_t^2}{2v_r^2} \quad (19)$$

and it is usually assumed to be positive,  $0 \leq \beta \leq 0.5$ . The asymmetry in our vicinity is related to the parameter  $x_0$  introduced above via the relation.

$$(20)$$

or

$$x_0 = x_s \sqrt{\frac{1-\beta}{\beta}} \quad (21)$$

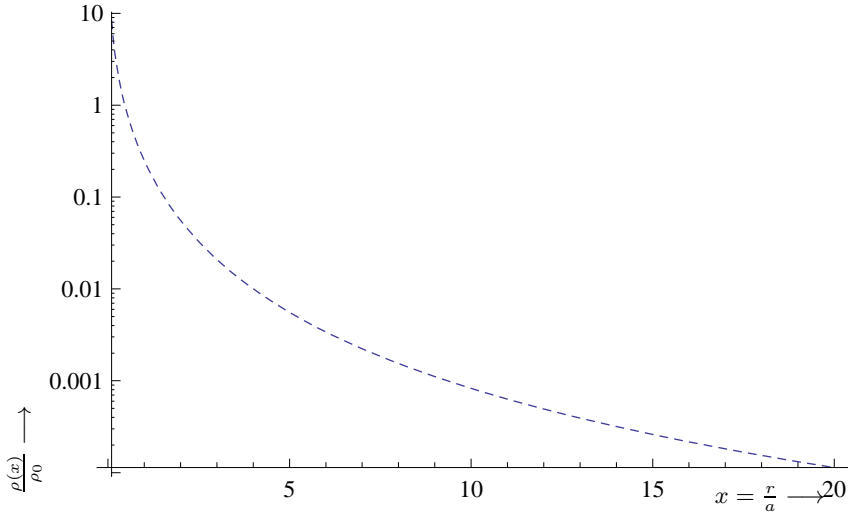


FIG. 3: The NFW dark matter density distribution in dimensionless units. The logarithmic scale is more convenient in this case, since this density diverges at the origin.

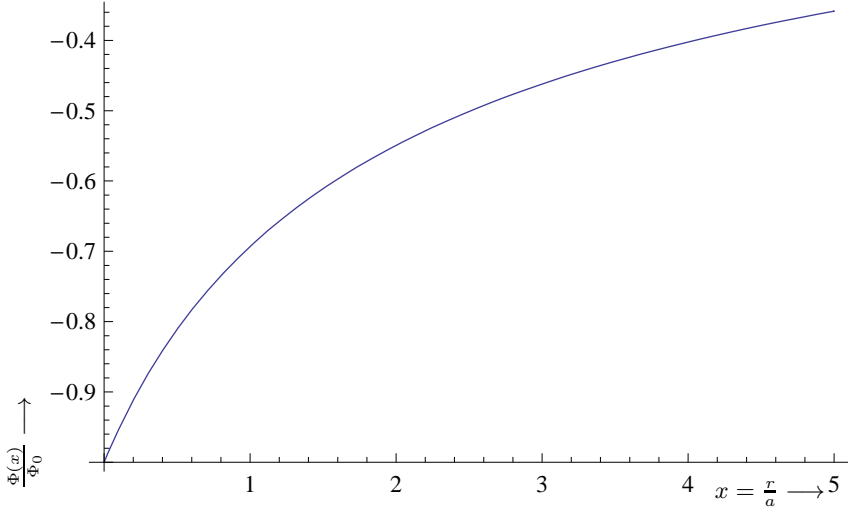


FIG. 4: The same as in Fig. 2 in the case of the NFW density.

Substitute the last expression in  $\tilde{\rho}(x, x_0)$  we get  $\tilde{\rho}(x, \beta)$ . In the case of the NFW profile [35] we get the results shown in Fig. 8.

The velocity distribution can be cast in the form:

$$f_v(y, \xi, \beta) = f_d(\Phi[x_s] + \frac{1}{2}y^2(1 + \beta(1 - \xi^2))), \quad y = \frac{v}{\sqrt{|\Phi_0|}}, \quad \xi = \cos \theta \quad (22)$$

Normalizing this function and integrating over the angles in the case of the NFW profile we get the velocity distribution shown in Fig. 9. It was a great surprise to us that this velocity distribution could be approximated by a Maxwell-Boltzmann distribution, which vanishes outside the range of  $y$  given by the exact distribution.

$$f_v^{MB} = C e^{-\frac{y^2(1 - \frac{2\beta}{3})(1 - \beta\xi^2)}{b^2(1 - \beta)}} \quad (23)$$



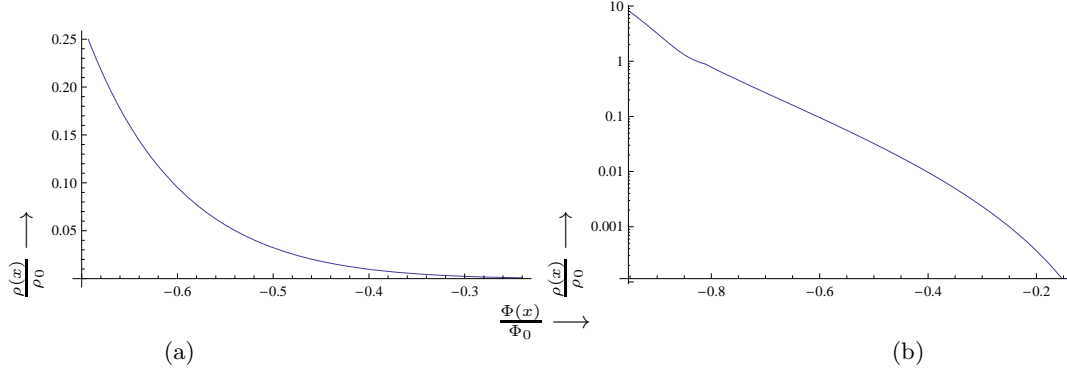


FIG. 7: The NFW density  $\frac{\rho}{\rho_0}$  as a function of the potential  $\frac{\Phi}{\Phi_0}$  (a). The same quantity on a logarithmic scale (b).

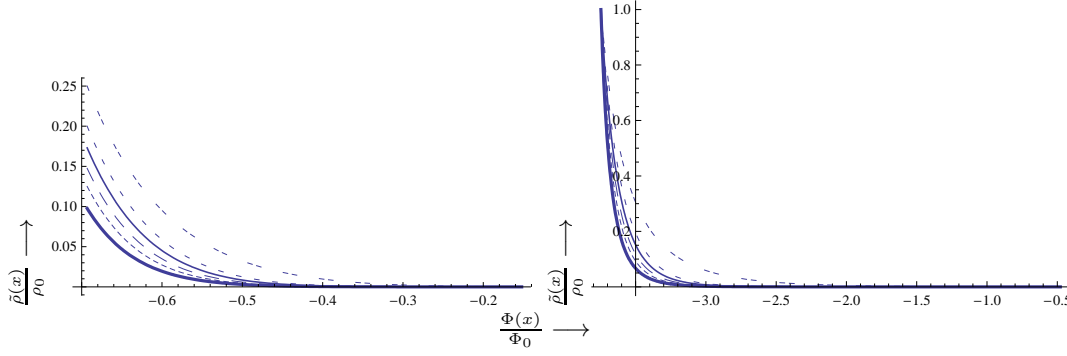


FIG. 8: The density  $\frac{\tilde{\rho}}{\rho_0}$  as a function of the potential  $\frac{\Phi}{\Phi_0}$  for various values of  $\beta$ , in the case of the NFW profile (a) and the VO profile (b). From top to bottom the asymmetry is increasing. The thick, dot-dot, dash-dash, fine, dot-dash and dot-long dash-dot lines correspond to  $\beta = 0.50, 0.40, 0.31, 0.22, 0.14$  and  $0$  respectively. The scales are different since in the VO case the density is finite at the maximum of the absolute value of the potential (the center of the profile), while in the NFW case it is not. Both of them as well as their derivatives up to third order vanish at the point the potential vanishes.

### TRANSFORMATION INTO OUR LOCAL COORDINATES.

We must now transform the above distributions from the galactic to the local coordinates.

$$f_v(y, \xi, \beta) \rightarrow f_v^{\text{local}}(y, \theta, \phi, \beta, \alpha, \delta, \gamma) = f_v^{\text{local}}\left(\frac{v}{v_0}, \theta, \phi, \beta, \alpha, \delta, \gamma\right) \quad (24)$$

This is accomplished by the substitutions:

$$y^2 \rightarrow X^2 + Y^2 + Z^2, \quad \xi^2 \rightarrow \frac{X^2}{X^2 + Y^2 + Z^2} \quad (25)$$

where

$$X = \frac{1}{sc}(y \cos \phi \sin \theta + \delta \sin \alpha), \quad Y = \frac{1}{sc}(y \sin \theta \sin \phi - \delta \cos \alpha \cos \gamma),$$

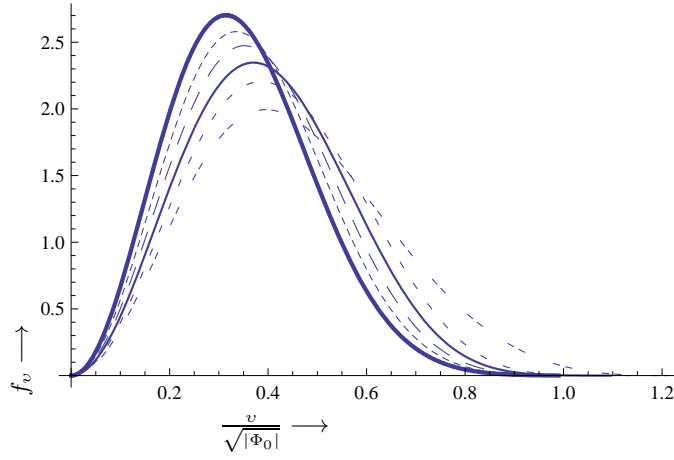


FIG. 9: The velocity distribution on our vicinity,  $4\pi y^2 f_v(y, \beta)$  as a function of the velocity in units of  $\sqrt{|\Phi_0|} = 5.2 \times 10^3 \text{ km s}^{-1}$ . Otherwise the notation is the same as in Fig. 8.

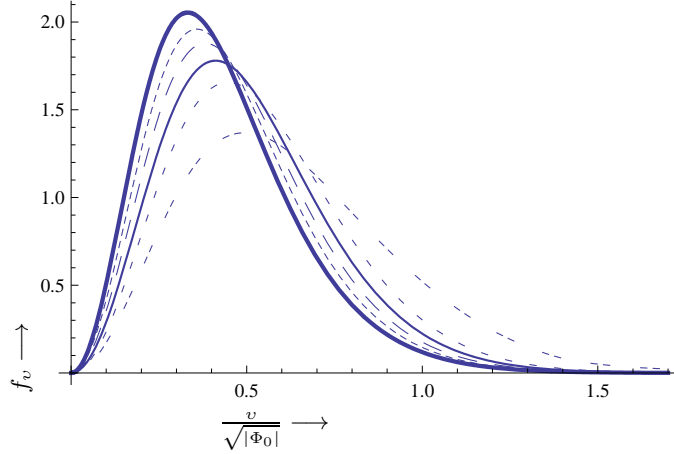


FIG. 10: The same as in Fig. 9 but the VO density profile. Here  $\sqrt{|\Phi_0|} = 5.5 \times 10^3 \text{ km s}^{-1}$ .

$$Z = \frac{1}{sc} (y \cos \theta + \delta \cos \alpha \sin \gamma + 1), \quad sc = \frac{\sqrt{2|\Phi(x_s)|}}{v_{\text{rot}}(x_s)} \approx 2.86 \quad (26)$$

where the now the polar axis has been chosen along the sun's direction of motion and the x-axes radially out of the galaxy.  $\delta = 0.135$  is the earth's rotational velocity in units of the sun's velocity,  $\gamma \approx \pi/6$  and  $\alpha$  is the phase of the earth ( $\alpha = 0$  around June the 3rd).

## A BRIEF DISCUSSION OF DIRECT WIMP EVENT RATES

Even though the expressions for the event rates for WIMP detection are well known for the reader's convenience we will include the basic formulas here in our own notation [15, 24, 36, 37]:

$$\left\langle \frac{dR}{du} \right\rangle = \frac{\rho(0)}{m_\chi} \frac{m}{Am_N} \sqrt{\langle v^2 \rangle} \int \frac{|v|}{\sqrt{\langle v^2 \rangle}} f_v^{\text{local}} \frac{d\sigma(u, v)}{du} d^3 \mathbf{v} \quad (27)$$

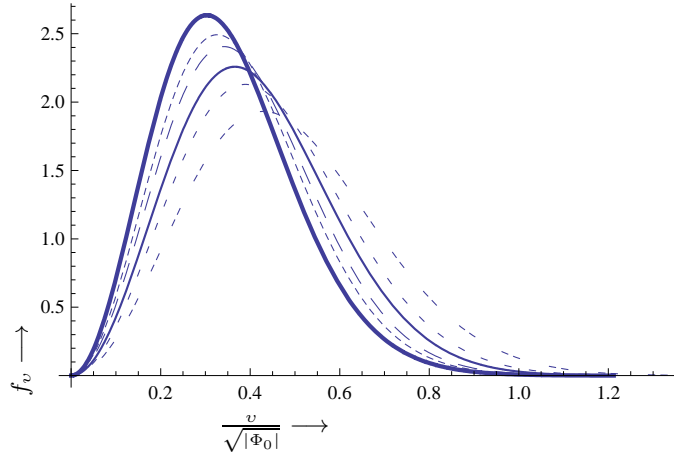


FIG. 11: The same as in Fig. 9 but using the approximate M-B velocity distribution.

The differential cross section is given by:

$$d\sigma(u, v) = \frac{du}{2(\mu_r b v)^2} [(\bar{\Sigma}_S F(u))^2 + \bar{\Sigma}_{spin} F_{11}(u)] \quad (28)$$

where  $u$  the energy transfer  $Q$  in dimensionless units given by

$$u = \frac{Q}{Q_0}, \quad Q_0 = [m_p A b]^{-2} = 40 A^{-4/3} \text{ MeV} \quad (29)$$

with  $b$  is the nuclear (harmonic oscillator) size parameter.  $F(u)$  is the nuclear form factor and  $F_{11}(u)$  is the spin response function associated with the isovector channel.

The scalar cross section is given by:

$$\bar{\Sigma}_S = \left( \frac{\mu_r(A)}{\mu_r(p)} \right)^2 \sigma_{p, \chi^0}^S A^2 \left[ \frac{1 + \frac{f_S^1}{f_S^0} \frac{2Z-A}{A}}{1 + \frac{f_S^1}{f_S^0}} \right]^2 \approx \sigma_{N, \chi^0}^S \left( \frac{\mu_r(A)}{\mu_r(p)} \right)^2 A^2 \quad (30)$$

(since the heavy quarks dominate the isovector contribution is negligible).  $\sigma_{N, \chi^0}^S$  is the LSP-nucleon scalar cross section. The spin cross section is given by:

$$\bar{\Sigma}_{spin} = \left( \frac{\mu_r(A)}{\mu_r(p)} \right)^2 \sigma_{p, \chi^0}^{spin} \zeta_{spin} \quad (31)$$

$\zeta_{spin}$  the nuclear spin ME.

Integrating over the energy transfer  $u$  we obtain the event rate for the coherent WIMP-nucleus elastic scattering, which is given by [15, 24, 36, 37]:

$$R = \frac{\rho(0)}{m_{\chi^0}} \frac{m}{m_p} \sqrt{\langle v^2 \rangle} \left[ f_{coh}(A, \mu_r(A)) \sigma_{p, \chi^0}^S + f_{spin}(A, \mu_r(A)) \sigma_{p, \chi^0}^{spin} \zeta_{spin} \right] \quad (32)$$

with

$$f_{coh}(A, \mu_r(A)) = \frac{100 \text{ GeV}}{m_{\chi^0}} \left[ \frac{\mu_r(A)}{\mu_r(p)} \right]^2 A t_{coh} (1 + h_{coh} \cos \alpha) \quad (33)$$

$$f_{spin}(A, \mu_r(A)) = \left[ \frac{\mu_r(A)}{\mu_r(p)} \right]^2 \frac{t_{spin} (1 + h_{spin} \cos \alpha)}{A} \quad (34)$$

In this work we will not be concerned with the spin cross section. The parameter  $t_{coh}$  takes into account the folding of the nuclear form factor with the WIMP velocity distribution,  $h_{coh}$  deals with the modulation due to the motion of the Earth and  $\alpha$  is the phase of the Earth (zero around June 2nd).

The number of events in time  $t$  due to the scalar interaction, which leads to coherence [38], is:

$$R \simeq 1.60 \cdot 10^{-3} \times \frac{t}{1\text{y}} \frac{\rho(0)}{0.3\text{GeVcm}^{-3}} \frac{m}{1\text{Kg}} \frac{\sqrt{\langle v^2 \rangle}}{280\text{km s}^{-1}} \frac{\sigma_{p,\chi^0}^S}{10^{-6} \text{pb}} f_{coh}(A, \mu_r(A)) \quad (35)$$

### The differential rate.

Before calculating the total event rates we like to say a few words about the differential rates (with respect to the energy transfer). In the notation of Eq. (33) we write:

$$\frac{dr}{du} = \frac{dt}{du} + \frac{dh}{du} \cos \alpha \quad (36)$$

where the first term gives the time average differential rate and the second the differential modulated rate. We can cast them in the form:

$$\frac{dt}{du} = \sqrt{\frac{2}{3}} a^2 F^2(u) \Psi_0(a\sqrt{u}), \quad \frac{dh}{du} = \sqrt{\frac{2}{3}} a^2 F^2(u) H(a\sqrt{u}) \cos \alpha. \quad (37)$$

where the two functions  $\Psi_0(a\sqrt{u})$  and  $H(a\sqrt{u})$  contain all the dependence on the velocity distribution. The energy transfer  $u$  is limited from below by the detector energy threshold and from above by the maximum WIMP velocity, i.e. :

$$u_{min} = \frac{Q_{th}}{Q_0} \leq u \leq u_{max} = \left( \frac{y_{max}}{a} \right)^2, \quad a = \left[ \sqrt{2} \mu_r b v_0 \right]^{-1}, \quad v_0 = \text{the sun's velocity} \quad (38)$$

Thus

$$r_{coh} = t_{coh} (1 + h_{coh} \cos \alpha) \quad (39)$$

$$t_{coh} = \int_{u_{min}}^{u_{max}} \frac{dt_{coh}}{du} du, \quad h_{coh} = \frac{1}{t_{coh}} \int_{u_{min}}^{u_{max}} \frac{dh_{coh}}{du} du. \quad (40)$$

We see that the modulation  $h$  is defined relative to the time average rate  $t$ . The above expressions manifestly show the essential parts:

- The elementary cross section.  
This is the most important part. It depends on two ingredients i) The particle model which provides the amplitude at the quark level and ii) The procedure for going from the quark to the nucleon level. We will not concern ourselves with such issues here.
- The WIMP density in our vicinity  $\rho_0$ .  
This has been obtained in two phenomenological density profile as described above.
- The dependence of the rate on the cross properties of the target and the WIMP mass.
- The quantity  $t$ .  
This is independent of the parameters of the particle model, except for the WIMP mass. It takes into account:

1. The nuclear structure effects (for the coherent process the nuclear form factor).

2. The WIMP velocity distribution.

This can be obtained from a given spherical density profile via the Eddington approach. In the present calculation we have included asymmetry by incorporating an angular momentum dependence in the phase space distribution. We find that the evaluation of WIMP direct detect detection rates can be simplified, since the obtained distribution can be approximated by a M-B distribution in a finite domain.

3. The energy threshold imposed by the detector. In the case of a non zero threshold the obtained rates depend on quenching. Such an effect will not be discussed here. The interested reader is referred to the literature (see e.g. [39]-[40])

- The quantity  $h$ .

This describes the modulation of the amplitude due to the Earth's velocity. It depends on the same parameters as  $t$ .

The evaluation of the quantities  $t$  and  $h$  with the obtained asymmetric velocity distribution will be discussed below.

## RESULTS

Since the NFW profile preceded the VO profile and is more widely known, we are going to employ the velocity distribution obtained with this profile to compute the direct WIMP detection rates.

### The differential rates

Before specializing our results to specific targets we remark that some of the effects of the velocity distribution are contained in the functions  $\Psi_0(x)$  and  $H(x)$  (see figs 12 and 13). The change in sign of  $H(x)$  partly explains why the modulation is smaller than what one would expect based on the parameter  $\delta$  (the velocity of the earth relative to that of the sun).

The precise differential rate depends, of course, on the target nucleus and the WIMP mass. Typical examples are shown in Figs 14-17.

### Total Rates

By integrating the differential rate we obtain the total rates. Typical examples for the coherent process are shown in Figs 18-21, for a typical light target ( $^{19}\text{F}$ ) and an intermediate-heavy target ( $^{127}\text{I}$ ).

## DISCUSSION

With the above ingredients we can now compute the total event rate. We will assume that the elementary nucleon cross section is independent of the WIMP mass and equal to  $10^{-6}\text{pb}$ . We will also take the WIMP density in our vicinity to be the popular value of  $0.3\text{ GeV cm}^{-3}$ , i.e. about half of what we found above from the rotation curves employing the NFW profile (the other half is assumed to be due to ordinary matter). Employing Eq. (35) and using the values of  $t$  indicated above at zero threshold we find the results shown in Figs. 22-23. There is no need to show again the effects of modulation on the rate, since the above shown results are adequate ( $h$  refers to the ratio of the modulated to the time averaged rate).

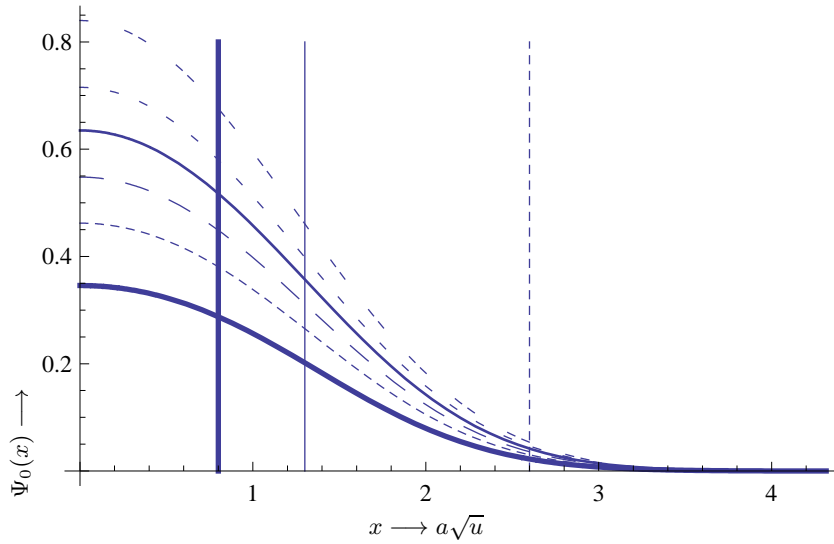


FIG. 12: The function  $\Psi_0(x)$  as defined in the text. Otherwise the notation is the same as in Fig. 8. Due to the nuclear form factor, not all the range of  $u$  is exploitable in direct WIMP detection. The high energy transfers are cut off due to the nuclear form factor at values lower than allowed by the kinematics. This is indicated by a dotted line, a fine line and a thick line for a WIMP mass of 30, 100 and 200 GeV respectively.

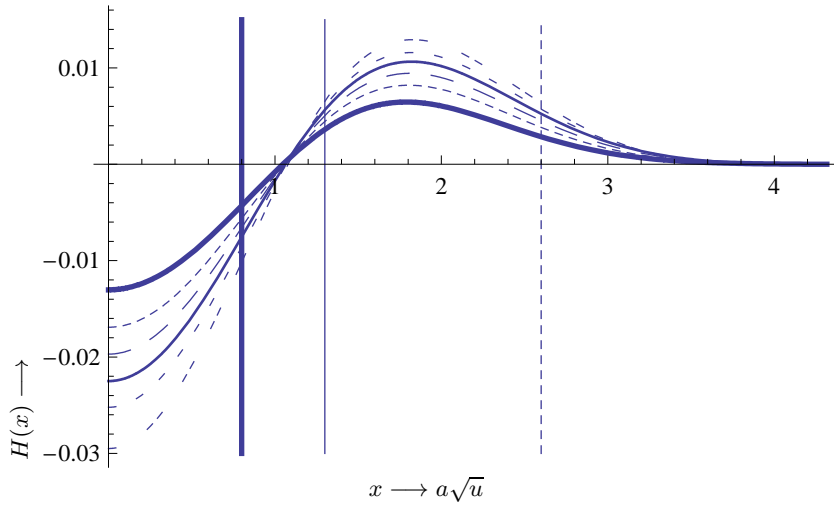


FIG. 13: The same as in Fig. 12 for the function  $H(x)$ . Note the change in sign as  $x$  increases.

## CONCLUSIONS

In the present paper we first derived the WIMP velocity distribution for a spherically symmetric WIMP density profile. This was done in a self consistent way by applying Eddington's approach. Asymmetry of the velocity distribution was also taken into account by incorporating angular momentum into the expression of the energy entering the phase space distribution function. Using this distribution function we obtained both the differential and total rates entering direct WIMP detection. We find that the time averaged differential rates do not sensitively depend on the asymmetry parameter  $\beta$ . The obtained shape of this signal unfortunately cannot really be differentiated from

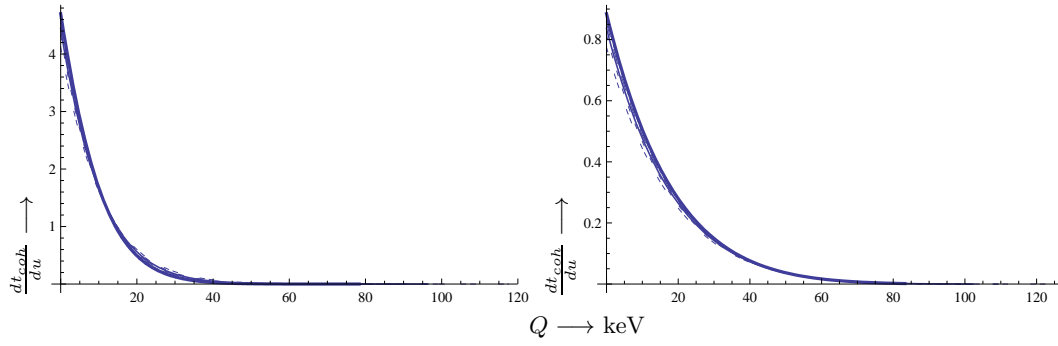


FIG. 14: On the left we show the differential rate  $\frac{dt_{coh}}{du}$  for  $m_\chi = 30$  GeV in the case of the axially symmetric distribution obtained in this work for a heavy nucleus. Here we have taken  $A=127$ . On the right we show the same quantity for  $m_\chi = 100$  GeV. Otherwise the notation is the same as in Fig. 8. The effect of the asymmetry is not visible. For the spin contribution the behavior is analogous.

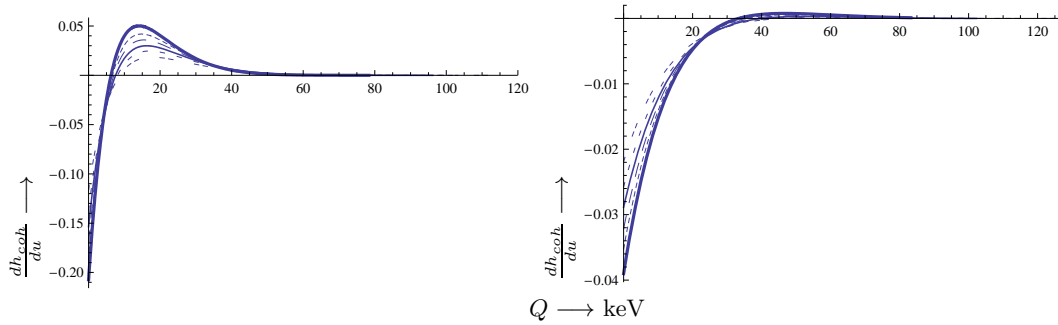


FIG. 15: The same as in Fig. 14 for the quantity  $\frac{dh_{coh}}{dQ}$ .

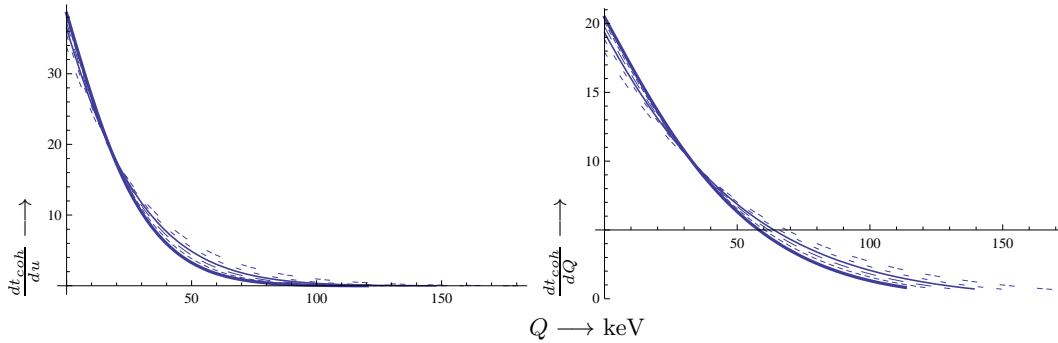


FIG. 16: On the left we show the quantity  $\frac{dt_{coh}}{du}$  for  $m_\chi = 30$  GeV in the case of the axially symmetric distribution obtained in this work for a light nucleus like  $A=19$ . On the right we show the same quantity for  $m_\chi = 100$  GeV. Otherwise the notation is the same as in Fig. 8. For the spin contribution the behavior is analogous.

that expected from most backgrounds. The differential modulation rate  $H$  shows some dependence

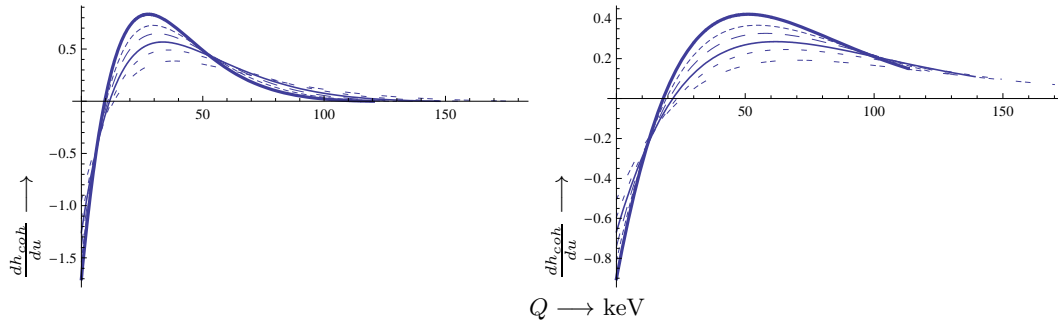


FIG. 17: The same as in Fig. 16 for the quantity  $\frac{dh_{coh}}{du}$ .

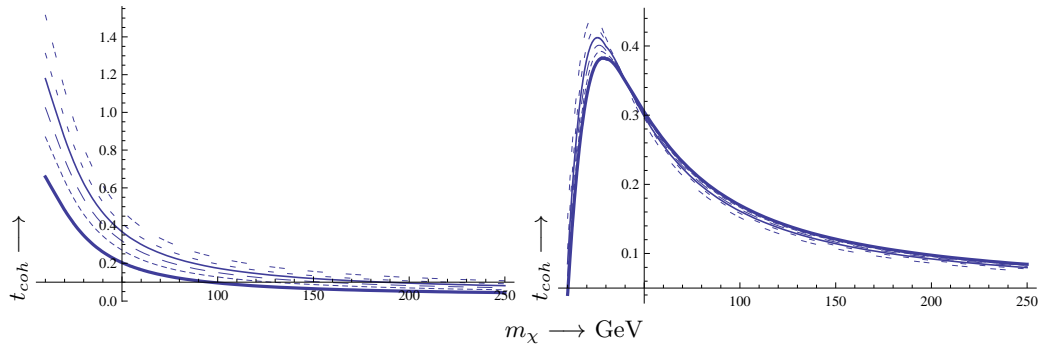


FIG. 18: On the left we show the rate  $t_{coh}$  as a function of the WIMP mass in the case of the axially symmetric distribution obtained in this work for a heavy nucleus. Here we have taken  $A=127$  and assumed zero threshold. On the right we show the same quantity for a threshold energy of 5 keV, Otherwise the notation is the same as in Fig. 8.

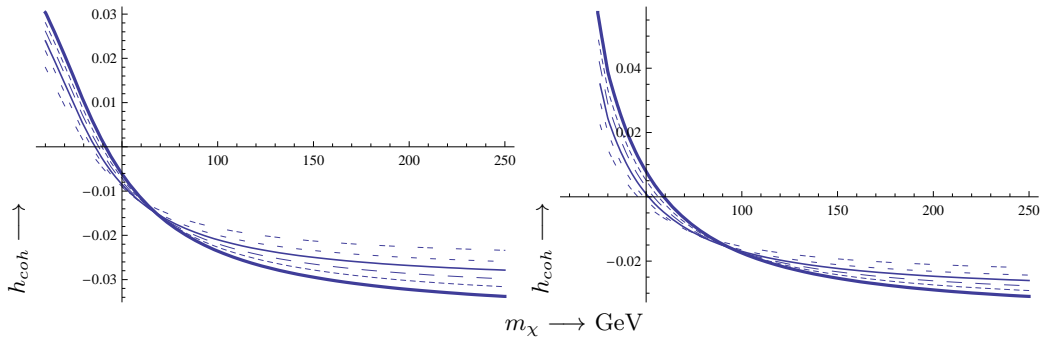


FIG. 19: The same as in Fig. 18 for the quantity  $h_{coh}$ .

on the asymmetry parameter, especially for light targets. We found that this differential rate changes sign at some energy transfer, which depends on the WIMP mass. Perhaps this signature may aid in discarding some season dependent backgrounds.

After that we computed the corresponding total rates. We find that the time averaged total rates are not very sensitive to the asymmetry parameter, in agreement with earlier results obtained with

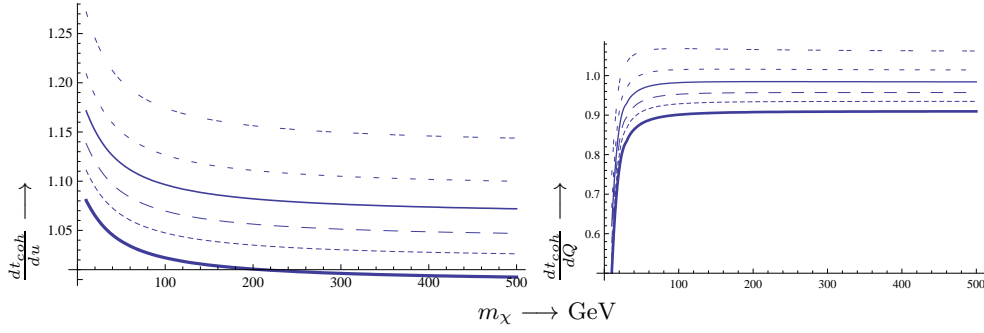


FIG. 20: On the left we show the quantity  $t_{coh}$  as a function of the WIMP mass in GeV in the case of the axially symmetric distribution obtained in this work for a light nucleus like  $A=19$ . On the right we show the same quantity for a threshold energy of 5 keV. Otherwise the notation is the same as in Fig. 8.

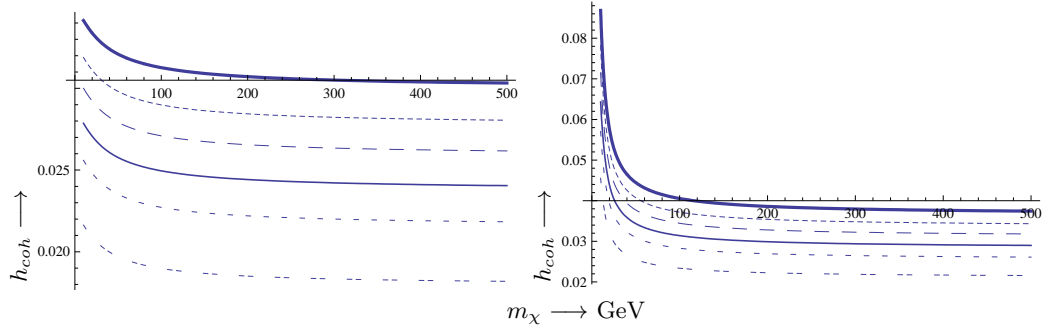


FIG. 21: The same as in Fig. 20 for the quantity  $h_{coh}$ .

distributions given in terms of Tsallis type functions [21]. The maximum rate is expected at a WIMP mass of about 75 GeV for a heavy target and 30 GeV for a light target. The modulation for a light system is always positive (maximum in June) and tends to increase with asymmetry. For zero threshold is rising from  $2h = 4\%$  to about  $2h = 6\%$  as the asymmetry increases from  $\beta = 0$  to  $\beta = 0.5$ . Assuming a threshold of 5 keV we get  $2h = 5 - 8\%$ . Higher modulations up to 16% can be expected at smaller WIMP masses. For a heavy target the modulation increases with asymmetry, but it goes through zero at a WIMP mass of about 50 GeV. We expect a positive modulation at lower WIMP masses, with a maximum of about  $2h = 6\%$  and negative modulation in the case of heavier WIMPS ranging to  $2|h| = 4$  to 6% depending on the asymmetry parameter.

Finally we were pleasantly surprised to find that both the spherically symmetric and the axially symmetric velocity distributions obtained from the realistic NFW density profile can be approximated by a Maxwell-Boltzmann velocity distribution in a finite domain, i.e. one in which the upper bound of the velocity (escape velocity) is not put in by hand but it comes naturally from the Eddington method. So one may use this distribution in the future to simplify the calculations.

We did not consider in this work directional experiments, i.e. experiments in which not only the energy but the direction of the recoiling nucleus is also observed [41]. In such experiments both the observed time averaged rates as well as the modulation are expected to be direction dependent [42]. We expect that such experiments are going to be much more sensitive to the form of the velocity distribution and, in particular, the asymmetry parameter.

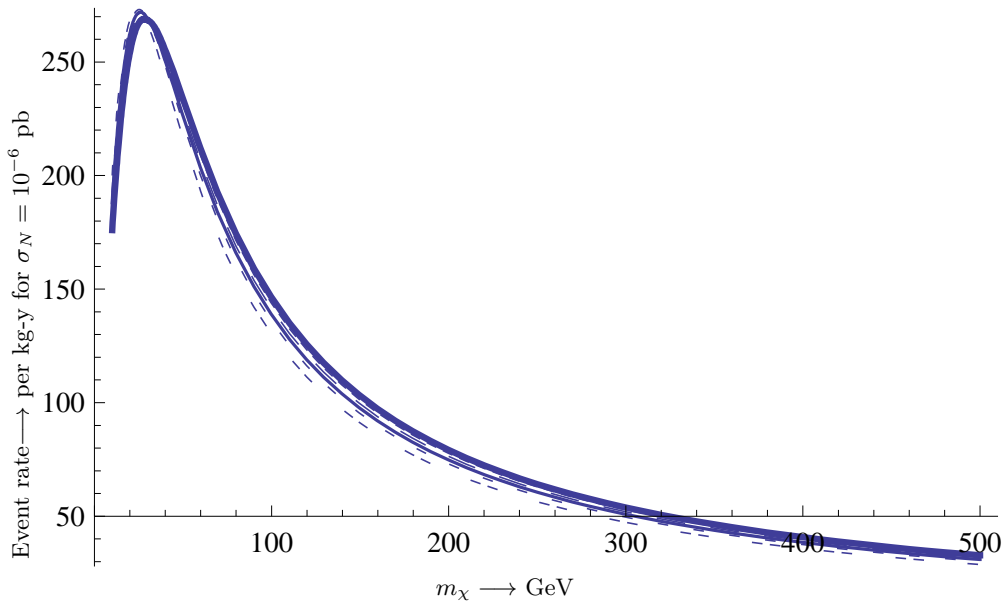


FIG. 22: The (time averaged) event rate per kg target per year as a function of the WIMP mass in GeV assuming a nucleon cross section  $\sigma_N = 10^{-6}$  pb. The results shown are due to the coherent mode for a heavy target ( $A=127$ ) and zero threshold. The effect of the asymmetry is not clearly visible. At low WIMP masses the rate is suppressed due to small reduced mass.

### Acknowledgments

This work was partly supported by the European Union under the contracts MRTN-CT-2004-503369 and MRTN-CT-2006-035863 (UniverseNet).

- 
- [1] S. Hanary *et al.*: *Astrophys. J.* **545**, L5 (2000);  
J.H.P Wu *et al.*: *Phys. Rev. Lett.* **87**, 251303 (2001);  
M.G. Santos *et al.*: *Phys. Rev. Lett.* **88**, 241302 (2002).
  - [2] P. D. Mauskopf *et al.*: *Astrophys. J.* **536**, L59 (2002);  
S. Mosi *et al.*: *Prog. Nuc.Part. Phys.* **48**, 243 (2002);  
S. B. Ruhl *al.*, astro-ph/0212229 and references therein.
  - [3] N. W. Halverson *et al.*: *Astrophys. J.* **568**, 38 (2002)  
L. S. Sievers *et al.*: astro-ph/0205287 and references therein.
  - [4] G. F. Smoot *et al.* (COBE Collaboration), *Astrophys. J.* **396**, L1 (1992).
  - [5] A. H. Jaffe *et al.*, *Phys. Rev. Lett.* **86**, 3475 (2001).
  - [6] D. N. Spergel *et al.*, *Astrophys. J. Suppl.* **148**, 175 (2003).
  - [7] D. P. Bennett *et al.*, *Phys. Rev. Lett.* **74**, 2867 (1995).
  - [8] M. W. Goodman and E. Witten, *Phys. Rev. D* **31**, 3059 (1985).
  - [9] J. Ellis and L. Roszkowski, *Phys. Lett. B* **283**, 252 (1992).
  - [10] A. Bottino *et al.*, *Phys. Lett B* **402**, 113 (1997).  
R. Arnowitt. and P. Nath, *Phys. Rev. Lett.* **74**, 4592 (1995); *Phys. Rev. D* **54**, 2374 (1996);  
hep-ph/9902237;  
V. A. Bednyakov, H.V. Klapdor-Kleingrothaus and S.G. Kovalenko, *Phys. Lett. B* **329**, 5 (1994).
  - [11] T. S. Kosmas and J. D. Vergados, *Phys. Rev. D* **55**, 1752 (1997).
  - [12] J. D. Vergados, *J. of Phys. G* **22**, 253 (1996).
  - [13] M. Drees and M. M. Nojiri, *Phys. Rev. D* **48**, 3843 (1993); *Phys. Rev. D* **47**, 4226 (1993).
  - [14] T. P. Cheng, *Phys. Rev. D* **38**, 2869 (1988); H-Y. Cheng, *Phys. Lett. B* **219**, 347 (1989).
  - [15] J. D. Vergados, On The Direct Detection of Dark Matter- Exploring all the signatures of the neutralino-

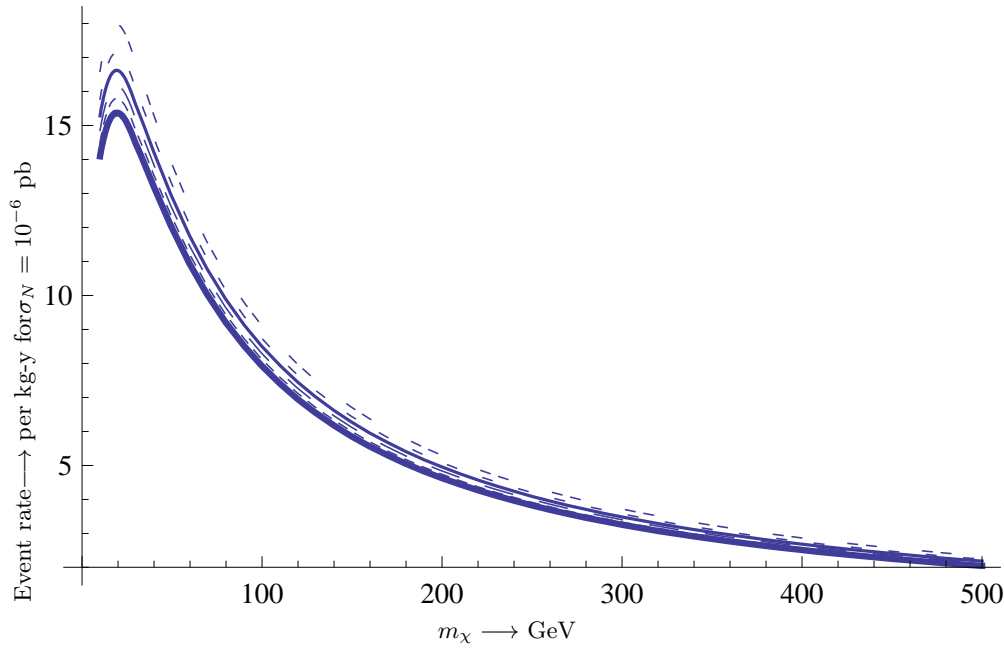


FIG. 23: The same as in Fig. 22 in the case of a light target ( $A=19$ ). The obtained rate slightly decreases with the asymmetry parameter.

nucleus interaction, hep-ph/0601064.

- [16] J. Ellis, M. Karliner, Spin Structure Functions, CERH-TH 7072/93.
- [17] M. T. Ressell *et al.*, *Phys. Rev. D* **48**, 5519 (1993); M.T. Ressell and D. J. Dean, *Phys. Rev. C* **56**, 535 (1997).
- [18] P. C. Divari, T. S. Kosmas, J. D. Vergados, and L. D. Skouras, *Phys. Rev. C* **61**, 054612 (2000).
- [19] A. K. Drukier, K. Freeze and D. N. Spergel, *Phys. Rev. D*, **33**, 3495 (1986);  
J.I. Collar *et al.*, *Phys. Lett B* **275**, 181 (1992).
- [20] J. D. Vergados, *Phys. Rev. D* **62**, 023519 (2000).
- [21] J. Vergados, S. N. Hansen, and O. Host, *Phys. Rev. D* **77**, 023509 (2008).
- [22] P. Sikivie, *Phys. Rev. D* **60**, 063501 (1999).
- [23] P. Sikivie, *Phys. Lett. B* **432**, 139 (1998).
- [24] J. D. Vergados, *Phys. Rev. D* **63**, 06351 (2001).
- [25] A. M. Green, *Phys. Rev. D* **63**, 103003 (2001).
- [26] G. Gelmini and P. Gondolo, *Phys. Rev. D* **64**, 123504 (2001).
- [27] C. Copi, J. Heo, and L. Krauss, *Phys. Lett. B* **461**, 43 (1999).
- [28] A. M. Green, *Phys. Rev. D* **66**, 083003 (2002).
- [29] A. S. Eddington, *NRAS* **76**, 572 (1916).
- [30] D. Merritt, *A J* **90**, 1027 (1985).
- [31] P. Ullio and M. Kamionkowski, *JHEP* **0103**, 049 (2001).
- [32] D. Owen and J. D. Vergados, *Astrophys. J.* **589**, 17 (2003), astro-ph/0203923.
- [33] J. Vergados and D. Owen, *Phys. Rev. D* **75**, 043503 (2007).
- [34] J. Binney, S. Tremain, *Galactic dynamics*, Princeton University Press.
- [35] C. F. J.F. Navarro and S. White, *ApJ* **462**, 563 (1996).
- [36] J. D. Vergados, *Phys. Rev. D* **57**, 103003 (2003), hep-ph/0303231.
- [37] J. D. Vergados, *J.Phys. G* **30**, 1127 (2004), 0406134.
- [38] N. Tetradis, J. Vergados, and A. Faessler, *Phys. Rev. D* **75**, 023504 (2007).
- [39] J. Vergados and H. Ejiri, *Nuc. Phys. B* **804**, 144 (2008), ; hep-ex/0503029.
- [40] M. Fairbairn, T. Schwetz, Spin-independent elastic WIMP scattering and the DAMA annual modulation signal, arXiv:0808.0704.
- [41] The NAIAD experiment B. Ahmed *et al.*, *Astropart. Phys.* **19** (2003) 691; hep-ex/0301039  
B. Morgan, A. M. Green and N. J. C. Spooner, *Phys. Rev. D* **71** (2005) 103507; astro-ph/0408047.
- [42] J. Vergados and A. Faessler, *Phys. Rev. D* **75**, 055007 (2007).